JMEPEG (2008) 17:772–779
DOI: 10.1007/s11665-008-9200-1

1059-9495/$19.00

Synthesis & Characterization of PVA/STA Composite Polymer Electrolyte Membranes for Fuel Cell Application

Arfat Anis, A.K. Banthia, and S. Bandyopadhyay

(Submitted March 9, 2007; in revised form November 11, 2007)

Chemically cross-linked composite membranes consisting of poly(vinyl alcohol) (PVA) and silicotungstic acid (STA) have been prepared by solution casting and evaluated as proton-conducting polymer electrolytes. The proton conductivity of the membranes was investigated as a function of blending composition, cross-linking density, and temperature. The conductivity mechanism was investigated by using Impedance spectroscopy in the region between 40 Hz and 10 MHz. Membranes were also characterized by FTIR spectroscopy to confirm the crossl-inking reaction and differential scanning calorimetry (DSC) to assess the thermal stability. Membrane swelling decreased with increase in cross-linking density accompanied by improvement in mechanical properties. The proton conductivity of the membranes was of the order of 10^{-3} S/cm and showed similar resistance to methanol permeability as Nafion 117 under the same measurement conditions.

Keywords advanced characterization, energy, polymer matrix composites

1. Introduction and Scope/Aim

Electricity is the fastest growing form of energy. Although it is being used more efficiently, and despite progress having been made in switching to fuels other than oil, the electricity industry still faces a number of major challenges, one of the most important of which is public concern about the environmental impact of electricity generation and use. Greater diversification of energy sources is required, with reduced associated emissions.

Fuel cells, in general, are attractive because they provide an innovative alternative to current power sources with higher efficiencies, renewable fuels, and a lower environmental cost. Fuel cells will contribute to reducing the demands for fossil fuel and nuclear-derived energy, both in the power generation sector and the road transport sector.

Fuel cells offer high efficiency and the possibility of zero emission at the point of use. Fuel cell efficiency is not a single number; however, it is a function of the power density at which the fuel cell operates, and thus the optimum nominal efficiency depends on the fuel cell performance and its capital cost. The electrolyte is implicated in both these aspects. The function of the membrane in PEM fuel cells is two fold: proton conduction from the anode to the cathode, and effective separation of the anode and cathode gases. Perfluorosulfonic acid (PFSA) membrane is by far the most studied proton electrolyte for PEM fuel cells. Because of its poly(tetrafluoroethylene) backbone, it is chemically inert in both oxidizing and reducing atmospheres. PFSA membranes are highly acidic and have excellent proton conductivity and good stability in a fuel cell environment. Despite these attributes, much research has been carried out over the past decade on exploring the possibilities of hydrocarbon-based membranes as proton electrolytes for PEM and direct methanol fuel cells (DMFC). Most importantly, PFSA membranes are limited in their temperature range of operations to around 80 °C; they have poor barrier properties to methanol, allowing methanol crossover from the anode to the cathode in a DMFC; high osmotic drag, which makes water management at high current densities difficult; and from the standpoint of recycling of the components of membrane-electrode assemblies (MEAs), the perfluorinated composition might become a future issue. These features are common to other perfluorinated membranes, such as those produced by Dow, Asahi Glass, and Asahi Chemical.

Polymer electrolytes have received extensive attention, especially for polymer electrolyte membrane fuel cells (PEMFCs). As alternatives to the currently available PFSA membranes, the newly developed polymer membrane electrolytes can be classified according to the way they are prepared. Most of the conventional polymers can be modified by attaching charged units within their structures and in this way obtain the ionic conductivity. The charged unit is commonly an anion, typically sulfonate ($-SO_3^-$) as in the sulfonated hydrocarbon polymers, e.g., polysulfone (PSF) (Ref 1), polyetheretherketone (PEEK) (Ref 2), and polybenzimidazole (PBI) (Ref 3-6).

The second method is to incorporate a polymer matrix with solid inorganic compounds, the so-called inorganic-organic composites or hybrids. Typical polymers in this group include polymers without functional groups such as polyethylene oxides (PEO) (Ref 7) and PBI (Ref 8-10) and polymers with functional groups such as PFSA (Ref 11), sulfonated polysulfone (SPSF) (Ref 12), and sulfonated polyetheretherketone (SPEEK) (Ref 13). The solid inorganic compounds include oxides such as amorphous silica and inorganic proton

Arfat Anis and **A.K. Banthia**, Materials Science Centre, Indian Institute of Technology, Kharagpur, India; and **S. Bandyopadhyay**, School of Materials Science & Engineering, University of New South Wales, Sydney, Australia. Contact e-mail: ajitbanthia2000@yahoo.co.in.

conductors such as zirconium phosphate (ZrP), ($Zr(HPO_4)_2 \cdot nH_2O$), phosphotungstic acid (PWA), ($H_3PW_{12}O_{40} \cdot nH_2O$), and silicotungstic acid (SiWA), ($H_4SiW_{12}O_{40} \cdot nH_2O$).

The third method is via chemical interactions between basic polymers and strong acids (Ref 14-16) or polymeric acids (Ref 17). Earlier studies employed basic polymers such as PEO, polyvinyl acetate (PVAc), polyacrylamide (PAAM), and polyethyleneimine (PEI). Most of these acid-doped polymers exhibit proton conductivity less than 10^{-3} S/cm at room temperature. High acid contents result in high conductivity but sacrifice mechanical stability, especially at temperatures above 70-80 °C. To improve the conductive, thermostable, and mechanical properties of the acid/polymer membranes, cross-linked polymers (e.g., PEI (Ref 18)), thermally stable polymers (e.g., polyoxadiazole (POD) (Ref 19) and PBI (Ref 14-16)), and introduction of inorganic fillers or/and plasticizers (Ref 8, 20) have recently been investigated.

In this work we have explored the suitability of polyvinyl-alcohol (PVA) for preparing inorganic-organic composite membranes by incorporating silicotungstic acid in the polymer matrix. PVA is a possible candidate because of its good chemical stability, film-forming ability, and high hydrophilicity and availability of cross-linking sites to create a stable membrane with good mechanical properties and selective permeability to water. PVA is a water-soluble polymer that readily reacts with different cross-linking agents to form gel. PVA is also biocompatible and biodegradable, and is widely used in medical, cosmetic, and packaging materials. For PVA, several cross-linking methods have been published for different uses, for example, chemically cross-linked PVAs are prepared by glutaraldehyde. PVA shows excellent insulation performance as a polymer material for pure dry materials; its conductivity can reach 10^{-10} to 10^{-14} S/cm. In these materials, the doping-impurity ions act as the primary electric carrier. PVA membranes have also been used in alcohol dehydration to break the alcohol-water azeotrope (Ref 21, 22), and due to its high selectivity for water to alcohol, it can effectively reduce the methanol crossover through the membrane when used in direct methanol fuel cells (DMFCs). In situ crosslinking of the hydroxyl functional groups available in PVA can effectively control the water uptake and hence the degree of swelling of the membranes. Optimizing the cross-linking density of the membranes can provide membranes with good mechanical properties. Cross-linking will also solve the problem of acid leaching from the membranes under hydrated conditions by effectively immobilizing the acid within the polymer matrix due to formation of the cross-linked networks. Composite membranes with different wt.% of silicotungstic acid and crosslink density were prepared and characterized by ATR-FTIR, Impedance spectroscopy (IS), methanol permeability measurements, and differential scanning calorimetry (DSC) to determine their suitability for use as proton-conducting polymer electrolytes for fuel cell applications.

2. Experimental

2.1 Materials and Membrane Preparation

PVA (Mw: 1,25,000 & degree of hydrolysis approx. 88%) and Glutaraldehyde (GA) (25% content in water) were obtained from s.d. fine-Chemicals Ltd. (Mumbai, India). Silicotungstic acid (STA) was obtained from Sisco Research Laboratories Pvt. Ltd (Mumbai, India). To prepare 5% (w/v) solution, PVA was dissolved in water at 80 °C with continuous stirring. To 20 g of 5 wt.% PVA solution, different amount of STA was added and the resulting mixture was stirred until a homogeneous solution was obtained. To this solution desired amount of the GA-cross-linking agent was added and the solution was further stirred for few minutes. After that the homogeneous solution was poured into a petri dish and allowed to dry at room temperature. The membranes obtained were 100 ± 10 μm in thickness.

2.2 Infrared Spectroscopy

Attenuated Total Reflection (ATR)-FTIR spectra in the range of 4000-400 cm^{-1} of the polymer-electrolyte films were measured with an FTIR Spectroscope (NEXUS-870, Thermo Nicolet Corporation) running Omnic software, and a uniform resolution of 2 cm^{-1} was maintained in all cases.

2.3 Impedance Spectroscopy

Conductivity measurements were made at room temperature (25 °C) after equilibrating the membrane in deionized water for 24 h. The membrane was sandwiched between stainless steel electrodes; ac impedance spectra of the membranes were obtained by using Agilent 4294A Precision Impedance Analyzer under an oscillation potential of 10 mV from 40 Hz to 10 MHz. The conductivity was calculated from the bulk resistance obtained from the high-frequency intercept of the imaginary component of impedance with the real axis. The conductivity of the membrane is determined by $\sigma = (1/R_b)$ (l/A), where R_b, l, and A represent bulk resistance, membrane thickness, and area of the electrode, respectively.

2.4 Methanol Permeability Measurement

Diffusion coefficient measurements were performed using an in-house-built diffusion cell having two compartments which were separated by the membrane situated horizontally. The donor compartment contains 50% v/v aqueous solution of methanol and the receptor compartment contains deionized water. Prior to measurements, the membranes were equilibrated in aqueous methanol solution 50% v/v for 24 h and the experiments were carried out at room temperature (25 °C). The methanol concentration of the receptor compartment was estimated using a differential refractometer (Photal OTSUKA Electronics, DRM-1021); the differential refractometer is highly sensitive to the presence of methanol. The change in refractive index of the diffusion samples was averaged over 52 scans in the differential refractometer to determine the change in refractive index.

2.5 Differential Scanning Calorimetry

A Perkin-Elmer DSC-6 was used for studying the melting and crystallization behavior of the polymeric membranes. The temperature and energy scales were calibrated with the standard procedures. The melting studies were performed in the temperature range of −30 to 200 °C at the heating rate of 10 °C/min in N_2 atmosphere.

2.6 Water Uptake

Water uptake of the composite membranes was determined by measuring the change in the weight before and after

hydration. The membrane was immersed in deionized water for 24 h at 25 °C, and the surface-attached water on the membrane was removed carefully by placing both the surfaces of the membranes gently over a filter paper. The weight of the wetted membrane was determined quickly using an analytical balance with a sensitivity of 0.1 mg. Water uptake was calculated by using the following equation:

$$\text{Water uptake} = \frac{M\text{w} - M\text{d}}{M\text{d}} \quad \text{(Eq 1)}$$

where M_w and M_d is the weight of the swollen polymer and the dry polymer in grams, respectively.

2.7 Dopant Loss

Titration method was used to determine the dopant loss from the membranes. Each composite membrane was soaked in 50 mL of deionized water for 24 h at ambient temperature. Then, 10 mL of the solution was titrated with 0.01 N NaOH. The dopant loss was calculated by using the following equation:

$$\text{DL} = \frac{A \times 0.01 \times 5}{m} \quad \text{(Eq 2)}$$

where DL is the dopant loss (meq./g), A the NaOH used to neutralize the resulting aqueous solution after equilibration (mL), 0.01 the normality of the NaOH, 5 the factor corresponding to the ratio of the amount of water taken to equilibrate the polymer to the amount used for titration, and m the sample mass (g).

2.8 Mechanical Properties

The tensile testing of the composite membranes was carried out using Hounsfield H10KS tensile-testing machine at a cross-head speed of 12.5 mm/min, temperature of 27 °C, and 75% humidity. The gauge dimension of the dog-bone-shaped test samples was 5 mm × 50 mm and each membrane was tested in triplicate.

3. Results and Discussions

3.1 FTIR Analysis

Figure 1(a) presents a comparison of the FTIR spectra of pure STA and the composite polymer electrolyte membrane. According to the assignments of Rocchiccioli-Deltcheff et al., the four absorption bands at 980, 924, 882, and 776 cm^{-1} are assigned to ν (W-O_d-W), ν (Si-O_a-W), ν (W-O_b-W), and ν (W-O_c-W), respectively. The bands in the IR spectrum of the membranes correspond well to those of STA, showing the typical features of Keggin anions. The most pronounced change, which appears in the spectra, is the shift of the W-O_c-W stretching-mode peak toward higher wave numbers in the composite polymer electrolyte membranes (PEMs) and the observed effect is stronger for PEMs with lower acid concentration. Similar behavior has been observed for many STA-containing systems, e.g., for SiO_2-STA composites (Ref 2) and is presumably due to the increase in the distance between the anions and hence the weakening of dipolar interactions. The increase in frequency may be explained as a consequence of a mixed, stretching bending character of this vibration. An upward shift is also observed for the W-O_b-W stretch, whereas bands ascribed to the Si-O_a-W and W-O_d-W stretching vibrations move to lower frequencies in the composite polymer electrolyte membranes.

Figure 1(b) shows the spectra of pristine PVA and cross-linked PVA-STA composite membrane; decrease in the absorbance of the peak at 3200-3400 cm^{-1} arises due to disappearance of the hydroxyl groups upon reaction with gluteraldehyde. The C-O-C stretching-mode peak shifts toward higher wave numbers in the composite PEM due to the formation of bound C-O-C of acetal ring and ether linkages as a result of the reaction between the hydroxyl groups and gluteraldehyde. From the spectral changes in Fig. 1(c), it can be seen that as the concentration of GA-cross-linking reagent content increases, more hydroxyl groups are consumed and more acetal rings and ether linkages are formed in the reaction between PVA and GA. The spectral changes in Fig. 1(d) show decrease in transmittance of the bands ascribed to STA with increase in STA content of the composite PEMs. From the study of IR spectra and well-known reaction mechanisms, typical products of the reaction between PVA and GA can be postulated as shown in Fig. 2.

3.2 Water Uptake

The water uptake of the composite PEMs as a function of STA content and cross link density of the membranes is shown in Fig. 3(a) and (b), respectively. Water uptake increases with increase in the STA content of the membranes up to 40 wt.% and further increase leads to decrease in the water uptake of the membrane. The increase in the water uptake with increase in the STA content is due to the hydrophilic nature of STA but after a certain critical level of doping there is decrease in the water uptake due to the resistance offered by the cross-linked networks to further uptake of water by the membrane.

Figure 3(b) shows the relationship between water uptake and cross-linking density of the composite membranes. The water uptake increases slightly with increase in cross-link density of the membrane from 0.47 to 0.94 mol% however, with further increase in cross-link density of the membrane the water uptake of the composite membranes decreased since the increasingly cross-linked networks formed at higher cross-link density restrict the swelling of the composite membranes due to water uptake.

3.3 Dopant Loss from Membranes

Apart from conductivity, the membrane to be used in fuel cell applications must fulfill a number of requirements including its stability in fuel cell environment. The major problem with composite membranes is the bleeding out of dopant from the polymer matrix. This phenomenon is investigated in the present study by determining the dopant loss from the PVA/STA composite membranes by titration method by soaking the membranes in water at room temperature for 24 h. The dopant loss values of the composite membranes are plotted against STA content and cross-linking density in Fig. 3(a) and (b), respectively. It can be seen that the STA loss increases continuously with increase in STA content of the composite PEMs. Dopant loss from the membranes initially slightly increased with the increase in the cross-linking density due to a similar trend in the water uptake of these membranes and STA loss from the membranes decreased with further increase in the cross-link density of the membranes (Table 1).

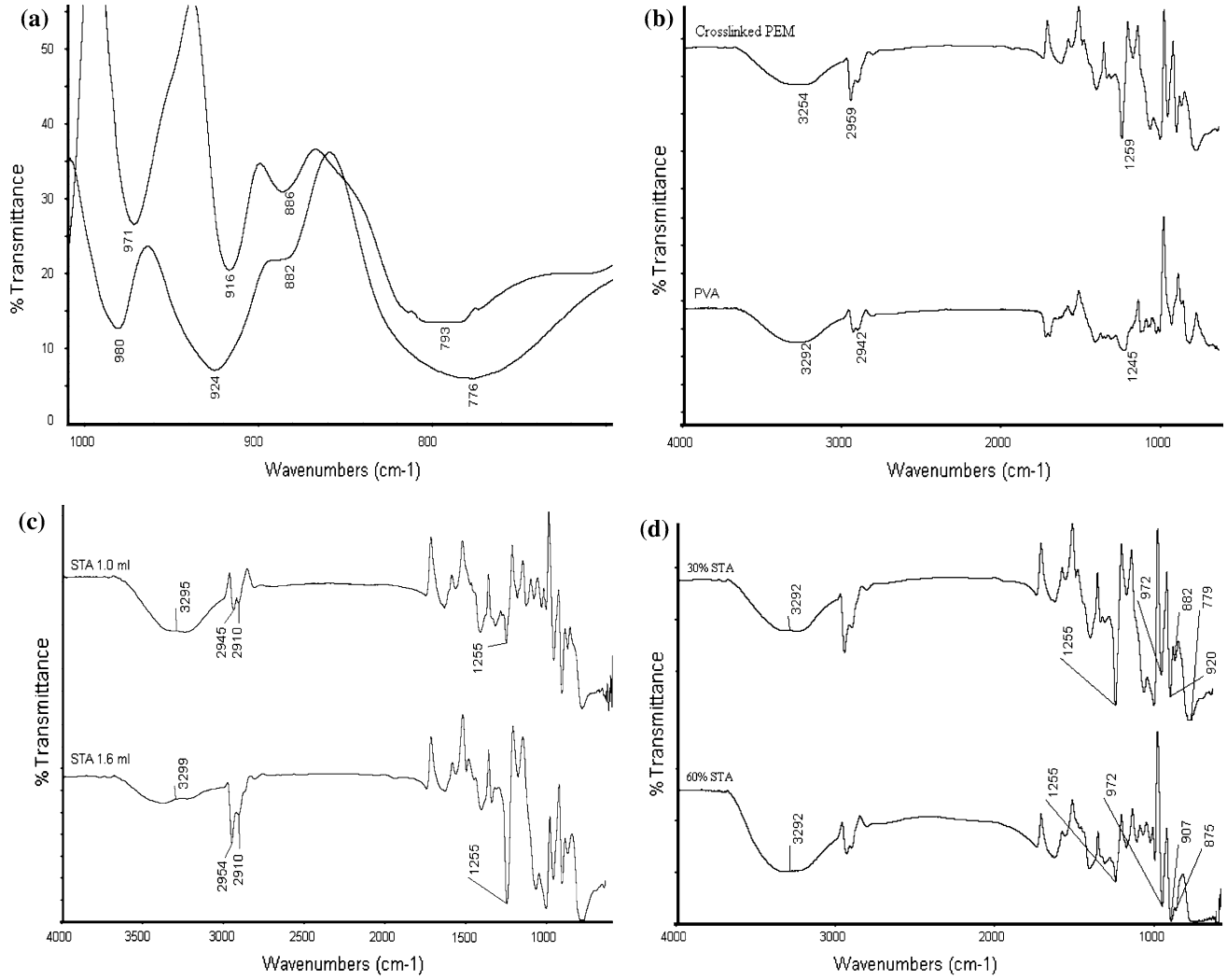

Fig. 1 (a) FTIR spectra of pure STA and the composite PEM. (b) FTIR spectra of pristine PVA and cross-linked PVA-STA composite membrane (c) FTIR spectra of the composite PEM with different cross-link density (d) FTIR spectra of the composite PEM with different STA content

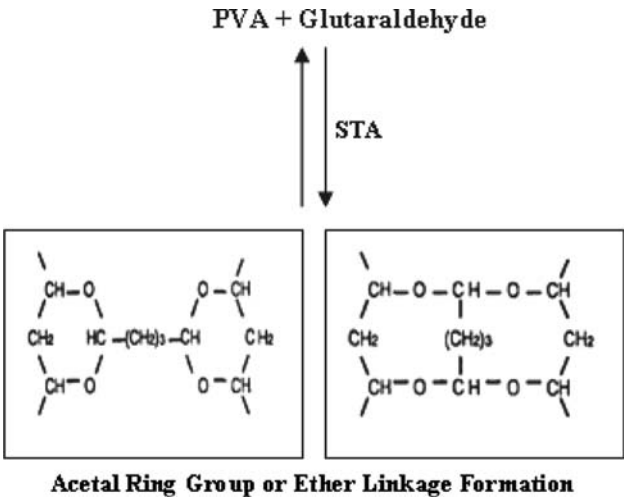

Fig. 2 Structure of cross-linked PVA formed by reaction between PVA and GA

3.4 Proton Conductivity Analysis

AC impedance spectroscopy was performed to determine the conductivity (σ) of these composite membranes. The result was plotted as a Cole-Cole plot to show the real/imaginary parts of the impedance at various frequencies. A typical Cole-Cole plot of a composite membrane sandwiched between stainless steel electrodes is shown in Fig. 4. The profile shows that the impedance decreases with increasing frequency. It indicates that the interfacial impedance decreases with increasing frequency, which can be attributed to double layer formation and charge transfer reaction.

Figure 5(a) shows the proton conductivity as a function of STA content. Here the proton conductivity was of the order of 10^{-3} S/cm. The proton conductivity increases sharply when the STA doped in the PVA matrix increased from 10 to 30 wt.%, and after that the conductivity decreased continuously with increases in STA content of the membranes. The membranes with more than 30-wt.% STA content showed a decrease in conductivity owing to the increase in dopant loss from these

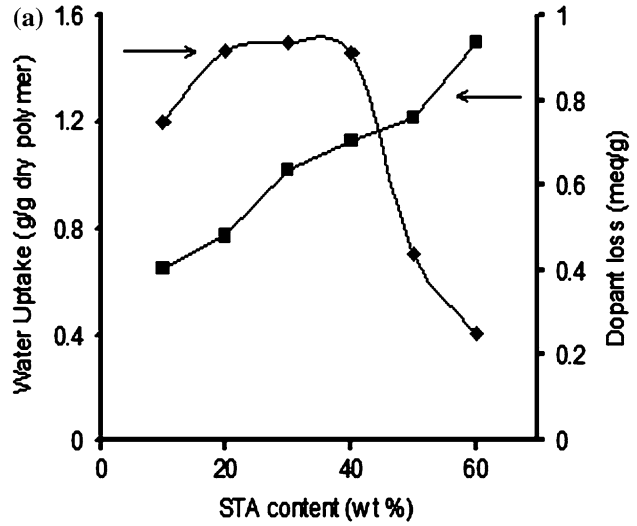

Fig. 3 (a) Water uptake and dopant loss of PVA/STA composite membranes with different STA content (b) Water uptake and dopant loss of PVA/STA composite membranes with different cross-link density

Table 1 Composition and properties of PVA/STA composite membranes

Membrane	STA, wt.%	Crosslink density, mol%	Conductivity, S/cm	Diff. coefficient, cm^2/s
STA-1	10	0.94	0.24×10^{-3}	1.71×10^{-6}
STA-2	20	0.94	1.05×10^{-3}	1.83×10^{-6}
STA-3	30	0.94	4.71×10^{-3}	1.84×10^{-6}
STA-4	40	0.94	3.75×10^{-3}	1.98×10^{-6}
STA-5	50	0.94	3.09×10^{-3}	2.42×10^{-6}
STA-6	60	0.94	2.42×10^{-3}	2.49×10^{-6}
STA-7	30	0.47	0.98×10^{-3}	1.66×10^{-6}
STA-8	30	1.40	0.96×10^{-3}	1.22×10^{-6}
STA-9	30	2.34	0.53×10^{-3}	1.27×10^{-6}
STA-10	30	3.77	1.52×10^{-3}	1.30×10^{-6}
Nafion-117	...	...	6.20×10^{-2}	6.50×10^{-6}

membranes. The drop in conductivity of the membrane clearly indicates that increase in the dopant content alone is not always the decisive factor to increase the proton conductivity, but one

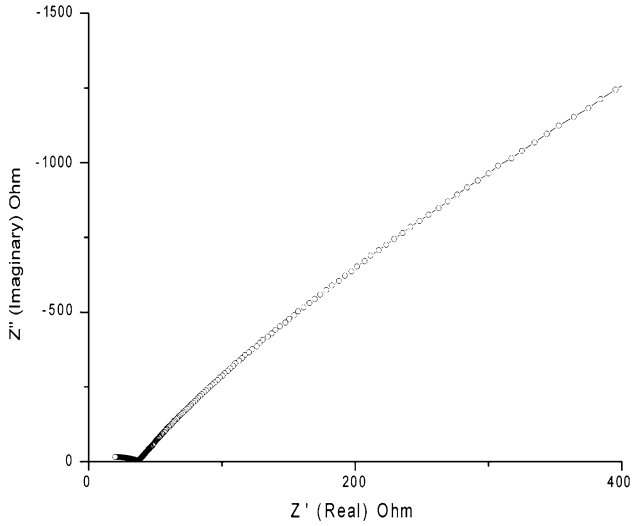

Fig. 4 Cole-Cole plot of the composite membrane, impedance frequency from 40 Hz to 10 MHz

has to consider water uptake and bleeding out of the dopant from the matrix while designing new membranes. A maximum conductivity of 4.71×10^{-3} S/cm was obtained for the membrane with 30 wt.% of STA in the PVA matrix.

Figure 5(b) shows the dependence of proton conductivity on the degree of crosslinking of the PVA matrix. The STA content was kept constant at 30 wt.% and the degree of crosslinking was varied from 0.47 to 3.74 mol%. Higher degree of crosslinking was limited due to the brittle nature of the composite membranes for practical use. The proton conductivity increased sharply with initial increase in cross-linking density but decreased with further increase in cross-link density of the membrane which is attributed to sharp decrease in water uptake of these membranes with increase in cross-link density.

The variation of conductivity with temperature for the different composite membranes is shown in Fig. 6. The Arrhenius plots of the temperature dependency of the conductivity exhibit convex upward curved profiles; therefore, experimental data have been fitted with the Vogel-Tamman-Fulcher (VTF) equation for conductivity for such electrolytic materials (not shown here). The VTF equation is $\sigma = \sigma_o \exp[-B/(T-T_0)$ where the constants σ_o (S/cm), $B(K)$, and $T_0(K)$ are adjustable parameters. Heteropolyacids exist in a series of hydrated phases, i.e., the structural unit of STA is $H_4SiW_{12}O_{40}\cdot nH_2O$, where the number of water molecules, n, might be in a range of 0-30, depending strongly on the temperature and RH. In the hydrated composite membranes the proton conduction is likely to happen by vehicular mechanism, rather than by Grotthuss mechanism, resulting in a long-range conductivity, with protons percolating through the sample.

3.5 Methanol Permeability

Figure 5(a) shows the methanol diffusion coefficient for the membranes as a function of STA content. The methanol diffusion coefficient was found to be 1.71×10^{-6} cm^2/s for the membrane with 10-wt.% STA content and increased continuously with increase in STA content of the membranes and reached a value of 2.49×10^{-6} cm^2/s for the membrane with 60-wt.% STA content. The terminal oxygen ($Mo{=}O_d$) of the polyanion not only can link together the hydrated hydrogen ions,

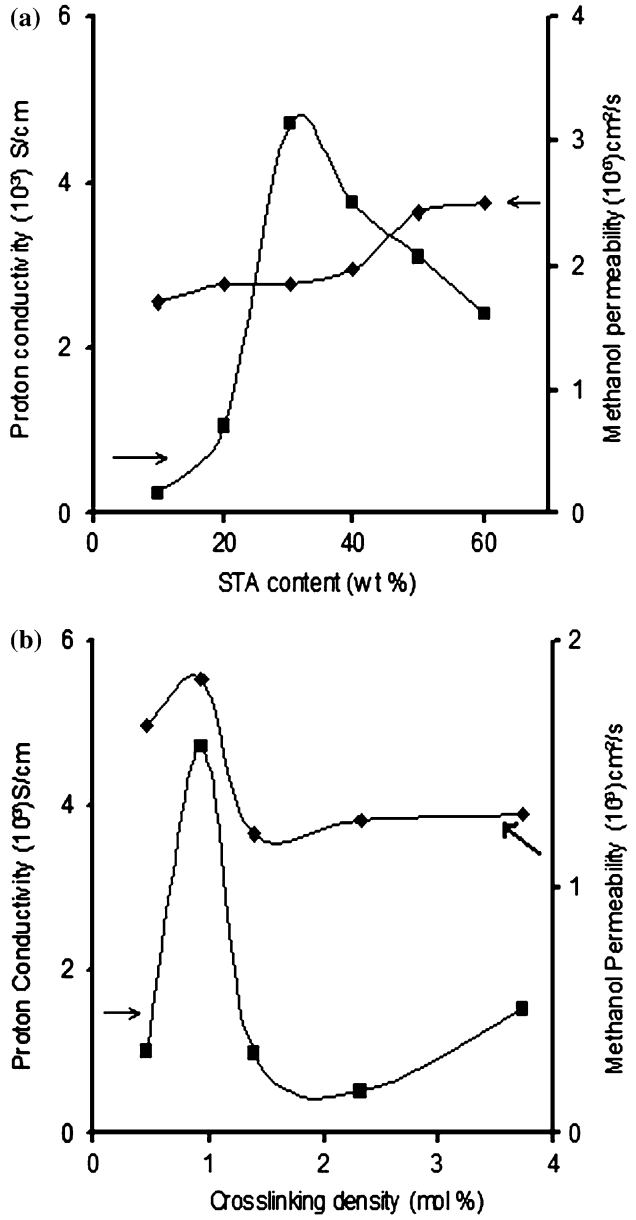

Fig. 5 (a) Proton conductivity and methanol permeability of PVA/STA composite membranes with different STA content (b) Proton conductivity and methanol permeability of PVA/STA composite membranes with different cross-link density

but also can connect to a small polar molecule such as methanol. With increase in the STA content, the probability of linking together the hydrated hydrogen ions and methanol would also increase, so that the conductivity and the methanol diffusion coefficient would increase at the same time. The increase in methanol diffusion coefficient and increase in proton conductivity do not follow the same trend. The increase of methanol diffusion coefficient and decrease in conductivity at higher STA content can be due to the formation of channels and pores in the membranes during equilibration. During equilibration the STA present on the surface of the membrane and that which could not be effectively immobilized in the polymer matrix are lost from the membranes, and this leads to the formation of these channels and pores in the composite membranes. The formation of these channels and pores in the membrane increases with increase in

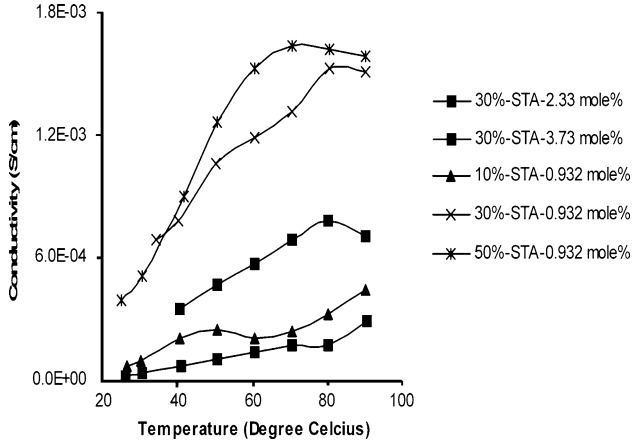

Fig. 6 Variation of conductivity with temperature for the composite membranes

the STA content of the membrane, as evident from the continuous increase in methanol diffusion coefficient and decrease in proton conductivity of the membranes.

Figure 5(b) shows the methanol diffusion coefficient for the membranes as a function of the cross-link density. The methanol diffusion coefficient was found to decrease from 1.66×10^{-6} cm^2/s to 1.30×10^{-6} cm^2/s with increase in cross-link density from 0.47 to 3.74 mol%. This decrease in diffusion coefficient is most likely due to the decrease in water uptake of the membranes and also due to decrease in STA loss from the membrane during equilibration. The STA is effectively immobilized in the polymer matrix due to the increase in the cross-link density of the membranes. The methanol diffusion coefficient for Nafion 117 reported in literature (Ref 10) is 6.5×10^{-6} cm^2/s determined under similar conditions and is used for comparison.

3.6 Differential Scanning Calorimetry

The DSC thermograms of the PVA/STA composite membranes are shown in Fig. 7. The thermograms show an

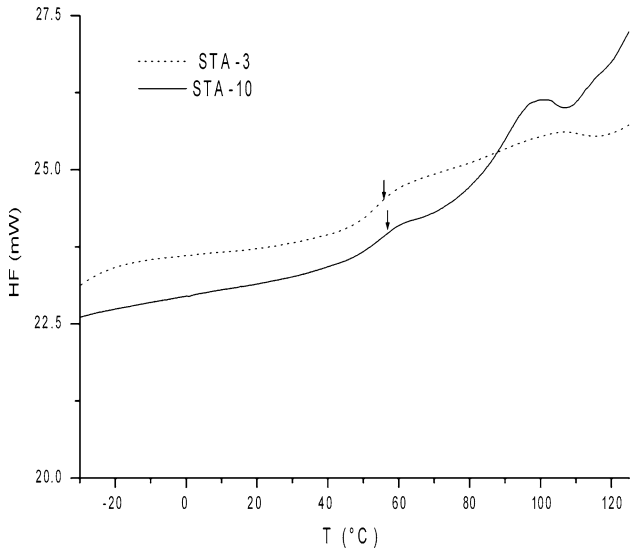

Fig. 7 DSC thermograms of the composite polymer electrolyte membranes

endothermic transition corresponding to the glass transition temperature of the composite membranes. The composite membrane with 30-wt.% STA and 0.94-mol% cross-link density shows a glass transition temperature (T_g) of 55.6 °C and that with 3.77 mol% cross-link density and same STA showed a slightly higher glass transition temperature of 56.9 °C, suggesting that the increase in cross-link density of the membranes restricts the mobility of the polymer chains resulting in increase of the glass transition temperature.

3.7 Mechanical Properties

The tensile strength and percent elongation at break of the composite membranes with different composition and cross-link density are shown in Fig. 8(a) and (b), respectively. The samples were tested in triplicate and the average values of tensile strength and percent elongation at break are reported. The tensile strength of 20 MPa and percent elongation of 480% was observed for uncross-linked pristine PVA membrane. Tensile strength of 15-50 MPa is observed for the composite membranes with different acid content, and the percent elongation for the composite membranes with different acid content increases with increase in acid content. This increase in percent elongation can be due to the esterification of the hydroxyl groups of PVA and hence results in reduction in the extent of hydrogen bonding between the hydroxyl groups of PVA.

The tensile strength of the composite membranes increases from 27 to 38 MPa with increase in cross-link density up to 2.34 mol% and then decreases with further increase in cross-link density, whereas the percent elongation at break decreases with increase in cross-link density. It can be seen that the cross-linked membranes exhibit higher tensile strength than the pristine PVA. This enhancement in tensile strength and decrease in percent elongation is due to the formation of cross-linked networks and hence restricted the mobility of the polymer chains.

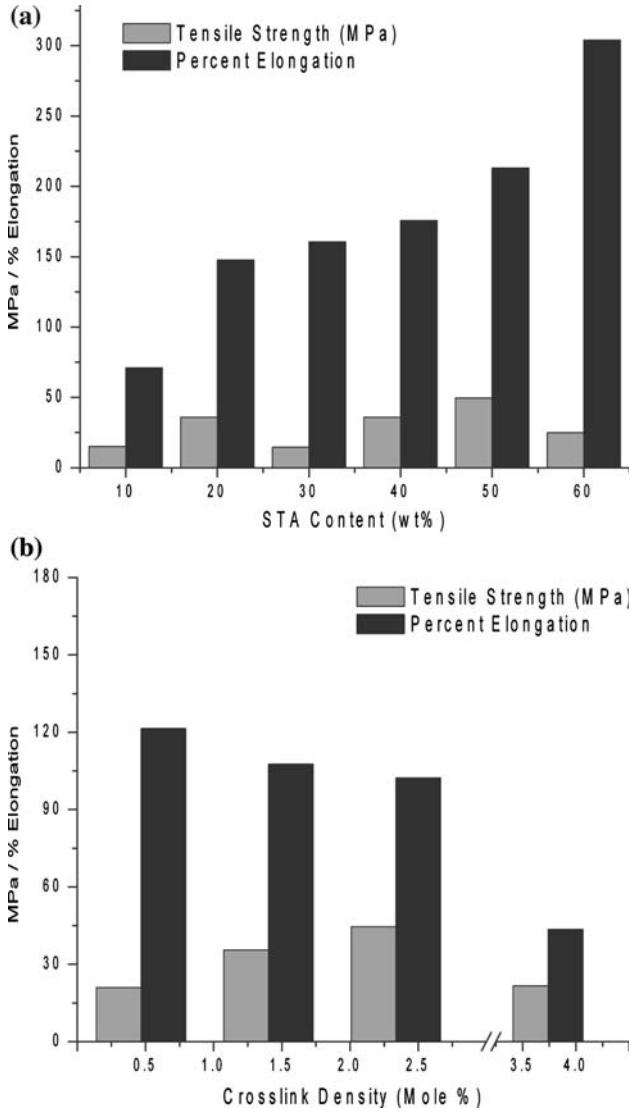

Fig. 8 (a) Tensile strength & Percent elongation of the composite polymer electrolyte membranes with different STA content (b) Tensile strength & Percent elongation of the composite polymer electrolyte membranes with different cross-link density membranes

4. Conclusion

The AC electrical response of the PVA-STA cross-linked proton conducting composite membranes has been investigated by using Impedance Spectroscopy in the frequency range 40 Hz to 10 MHz, between 25 and 90 °C.

(1) The highest proton conductivity of 4.71×10^{-3} S/cm was obtained for the membrane with 30 wt.% STA content with a cross-linking density of 0.94 mol% at room temperature which is an order lower to the currently used PFSA membranes.
(2) The lowest methanol permeability of 1.30×10^{-6} cm^2/s was obtained which is 5 times lower than that reported for the commercially available Nafion membranes under similar measurement conditions.
(3) FTIR results proved the formation of cross-linked networks.
(4) The composite membranes have good mechanical and thermal stability.

Furthermore, the PVA polymer used is biodegradable, nonhazardous, and environmentally benign. The present investigation suggests that these composite membranes if optimized may serve as a potential alternative proton-conducting membrane for polymer electrolyte membrane fuel cell applications.

References

1. F. Lufrano, I. Gatto, P. Staiti, B. Antonucci, and E. Passallacqua, Sulfonated Polysulfone Ionomer Membranes for Fuel Cells, *Solid State Ionics*, 2001, **145**(1–4), p 47–51, in English
2. J. Kerres, A. Ullrich, F. Meier, and T. Haïing, Synthesis and Characterization of Novel Acid-Base Polymer Blends for Application in Membrane Fuel Cells, *Solid State Ionics*, 1999, **125**(1–4), p 243–249, in English
3. R.J. Spry, M.D. Alexander Jr., S.J. Bai, T.D. Dang, G.E. Price, D.R. Dean, B. Kumar, J.S. Solomon, and F.E. Arnold, Anisotropic Ionic Conductivity of Lithium-Doped Sulfonated PBI, *J. Polym. Sci., Part B: Polym. Phys.*, 1997, **35**(17), p 2925–2933, in English
4. P. Staiti, F. Lufrano, A.S. Aricò, E. Passalacqua, and V. Antonucci, Sulfonated Polybenzimidazole Membranes—Preparation and

Physico-Chemical Characterization, *J. Membr. Sci.*, 2001, **188**(1), p 71–78, in English
5. J.-M. Bae, I. Honma, M. Murata, T. Yamamoto, M. Rikukawa, and N. Ogata, Properties of Selected Sulfonated Polymers as Proton-Conducting Electrolytes for Polymer Electrolyte Fuel Cells, *Solid States Ionics*, 2002, **147**(1,2), p 189–194, in English
6. D.J. Jones and J. Rozière, Recent Advances in the Functionalization of Polybenzimidazole and Polyetherketone for Fuel Cell Applications, *J. Membr. Sci.*, 2001, **185**(1), p 41–58, in English
7. I. Honma, Y. Takeda, and J.M. Bae, Protonic Conducting Properties of Sol-Gel Derived Organic/Inorganic Nanocomposite Membranes Doped with Acidic Functional Molecules, *Solid State Ionics*, 1999, **120**(1–4), p 255–264, in English
8. P. Staiti, M. Minutoli, and S. Hocevar, Membranes Based on Phosphotungstic Acid and Polybenzimidazole for Fuel Cell Application, *J. Power Sources*, 2000, **90**(2), p 231–235, in English
9. P. Staiti and M. Minutoli, Influence of Composition and Acid Treatment on Proton Conduction of Composite Polybenzimidazole Membranes, *J. Power Sources*, 2001, **94**, p 1–13, in English
10. P. Staiti, Proton Conductive Membranes Based on Silicotungstic Acid/Silica and Polybenzimidazole, *Mater. Lett.*, 2001, **47**(4–5), p 241–246, in English
11. P. Costamagna, C. Yang, A.B. Bocarsly, and S. Srinivasan, Nafion115/Zirconium Phosphate Composite Membranes for Operation of PEMFCs above 100 °C, *Electrochim. Acta*, 2002, **47**(7), p 1023–1033, in English
12. C. Poinsignon, I. Amodio, D. Foscallo, and J.Y. Sanchez, Low Cost Filled Thermostable Ionomer Membrane for PEMFC, *Mater. Res. Soc. Symp. Proc.*, 1999, **548**, p 307–312, in English
13. B. Bonnet, D.J. Jones, J. Rozière, L. Tchicaya, G. Alberti, M. Casciola, L. Massinelli, B. Bauer, A. Ieraio, and E. Ramunni, Hybrid Organic-Inorganic Membranes for a Medium Temperature Fuel Cell, *J. New Mater. Electrochem. Syst.*, 2000, **3**(2), p 87–92, in English
14. J.S. Wainright, J.-T. Wang, D. Weng, R.F. Savinell, and M. Litt, Acid-Doped Polybenzimidazoles: A New Polymer Electrolyte, *J. Electrochem. Soc.*, 1995, **142**(7), p L121–L123, in English
15. R. Bouchet and E. Siebert, Proton Conduction in Acid Doped Polybenzimidazole, *Solid State Ionics*, 1999, **118**(3,4), p 287–299, in English
16. M. Kawahara, J. Morita, M. Rikukawa, K. Sanui, and N. Ogata, Synthesis and Proton Conductivity of Thermally Stable Polymer Electrolyte: Poly(benzimidazole) Complexes with Strong Acid Molecules, *Electrochim. Acta*, 2000, **45**(8,9), p 1395–1398, in English
17. J.A. Kerres, Development of Ionomer Membranes for Fuel Cells, *J. Membr. Sci.*, 2001, **185**(1), p 3–27, in English
18. R. Tanaka, H. Yamamoto, A. Shono, K. Kubo, and M. Sakurai, Proton Conducting Behavior in Non-Crosslinked and Crosslinked Polyethylenimine with Excess Phosphoric Acid, *Electrochim. Acta*, 2000, **45**(8,9), p 1385–1389, in English
19. S.M.J. Zaidi, S.F. Chen, S.D. Mikhaikenko, and S. Kaliaguine, Proton Conducting Membranes Based on Polyoxadiazoles, *J. New Mater. Electrochem. Syst.*, 2000, **3**(1), p 27–32, in English
20. J.C. Lassègues, J. Grondin, M. Hernandez, and B. Marée, Proton Conducting Polymer Blends and Hybrid Organic Inorganic Materials, *Solid State Ionics*, 2001, **145**(1–4), p 37–45, in English
21. J.W. Rhim and Y.K. Kim, Pervaporation Separation of MTBE-Methanol Mixtures Using Cross-Linked PVA Membranes, *J. Appl. Polym. Sci.*, 2000, **75**(14), p 1699–1707, in English
22. W.Y. Chiang and C.L. Chen, Separation of Water—Alcohol Mixture by Using Polymer Membranes—6. Water—Alcohol Pervaporation Through Terpolymer of PVA Grafted with Hydrazine Reacted SMA, *Polymer*, 1998, **39**(11), p 2227–2233, in English